STRUCTURAL CONTROL AND HEALTH MONITORING
Struct. Control Health Monit. 2006; **13**:748–757
Published online 16 November 2005 in Wiley InterScience (www.interscience.wiley.com). DOI: 10.1002/stc.109

Application of a high-pressure gas semi-active resettable damper to the benchmark smart base-isolated building

John Leavitt, James E. Bobrow, Faryar Jabbari*,† and Jann N. Yang

Henry Samueli School of Engineering, University of California, Irvine, CA 92697, U.S.A.

SUMMARY

We discuss the application of a new class of low-cost and high-reliability semi-active devices for the response mitigation of structures subject to earthquakes. These devices, which manipulate stiffness rather than damping, are evaluated by the smart base-isolated benchmark building. The basic motivation, idealization as a stiffness resetting damper or device, development of control logic that ensures the semi-active property, and initial testing and validation results from recently developed prototypes are discussed. The principle idea allows the use of reliable and inexpensive hydraulic or pneumatic technologies, and leads to a decentralized and easy to implement architecture. The results from the benchmark simulations show performance competitive with well-known semi-active techniques. Copyright © 2005 John Wiley & Sons, Ltd.

KEY WORDS: resetting stiffness devices; semi-active control

1. INTRODUCTION

Base isolation systems, in particular elastomeric bearings, have been used on buildings and bridges to reduce the seismic response of the superstructure. Under near-field earthquakes, however, it has been shown that the drift of the rubber-bearing isolators may be excessive. Currently, the performance of base-isolated structures is enhanced by the use of passive energy dissipation devices, such as viscous dampers. A control system consisting of a combination of the base isolation system and control devices such as passive, active or semi-active control elements is often referred to as a hybrid control system and its performance has been investigated through a variety of means [1–5]. Such systems are also called smart base isolation systems [6–9].

Among different combinations that are possible for a hybrid approach, semi-active control systems are attractive for use with base isolation systems because of their mechanical simplicity,

*Correspondence to: Faryar Jabbari, Henry Samueli School of Engineering, University of California, Irvine, CA 92697, U.S.A.
†E-mail: fjabbari@uci.edu

Contract grant sponsor: National Science Foundation; contract grant number: CMS-0218813.

Received 13 December 2004
Revised 1 April 2005
Accepted 28 May 2005

low power requirements, and large controllable force capacity. There have been a number of studies on the performance of semi-active systems in controlling base-isolated buildings and bridges: with variable orifice fluid dampers [5,10], MR dampers [6,7], resettable semi-active stiffness dampers or devices [11–14], and semi-active friction devices [15,16]. Note that the discussion here is focused on semi-active control of base-isolated building and bridges, and for brevity the much wider literature on other semi-active control systems are omitted (the interested reader can consult [17] for a comprehensive review).

In this paper, we apply a new class of semi-active devices to the smart base-isolated benchmark building [8]. These resettable semi-active stiffness devices have been presented in [18,19] and their application to seismic excited buildings and bridges has been studied in several papers [20–22]. Recently, full-scale high-performance semi-active stiffness dampers using high-pressure gas have been designed, manufactured and tested [23,24]. Here we present preliminary experimental test results for the hysteretic behavior of these devices and show their performance—through numerical simulations—on the benchmark building [8] and compare the results with the sample MR controller in that reference. Following standard practice in the literature, throughout this paper, we interchangeably refer to the proposed resetting stiffness elements as devices or dampers (the latter with a slight abuse to notation since the proposed devices essentially manipulate stiffness and not damping).

2. MOTIVATION AND BASIC MODEL

The basic idea behind the proposed resetting devices is to develop dampers that act as a controllable spring (to manipulate structural stiffness), whose value can be changed in real time, either continuously or in a on/off type switching. Using standard hydraulic or pneumatic devices, we can obtain high stiffness values with off-the-shelf, relatively inexpensive and highly reliable components, and avoid the use of novel materials (and their corresponding costs and reliability issues). While the hardware configurations and general concepts can be applied to a more traditional form of variable stiffness, we focus on *resetting* of the stiffness; i.e. when the stiffness can be changed from the maximum value to zero and then increased back to the maximum value either immediately or as soon as possible.

Consider the schematic in Figure 1, in which a single degree of freedom system is connected to a resetting device. The device itself is presented as either a double-acting cylinder with an external line and an on/off valve (configuration a), or a linear spring connected to a support with a collar that can be locked or unlocked (configuration b).

In configuration (a), when the valve is closed, motion of the piston compresses the gas, and as shown in [21], the force produced by the gas can be closely approximated by a linear spring with stiffness as a function of piston area, initial pressure in the chamber, and cylinder volume. Once the valve is opened, gas (or fluids in a hydraulic device) will flow from one chamber to another, releasing stored energy as heat. Opening of the valve is thus analogous to unlocking the spring and allowing it to release its potential energy. In both cases, we can increase the stiffness (by closing the valve or locking the collar) once the energy is drained. Typically, the cylinder and valve analogy is a more realistic schematic, while the linear spring analogy allows for a simple model that can be used to develop semi-active control logic for the damper.

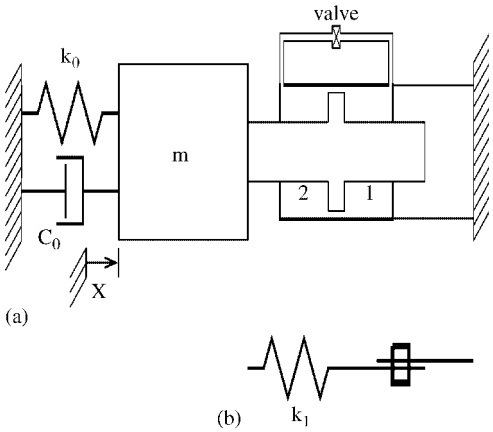

Figure 1. Schematic representing the resetting.

Consider the linear spring schematic. We denote the potentially time varying stiffness of the spring k_1 as

$$k_1(t) = \alpha(t)k_1, \quad \alpha = 0 \text{ or } 1$$

where α is used as the switching or control logic, i.e. $\alpha = 1$ means high stiffness $(k_0 + k_1)$ or closed valve, and $\alpha = 0$ devotes low stiffness (k_0) or an open valve. The collar can be unlocked at any time during the motion, which means that we set $\alpha = 0$. As long as the energy is drained, it can be locked, at which time the device or damper is 'reset' and α becomes one again.

Now consider the most recent instance of resetting, say at time t_1. We denote the position of the piston at the time of resetting as x_s, i.e. $x_s = x(t_1)$. From this point on, the energy in the spring is $\frac{1}{2}\alpha k_1(x - x_s)^2$. Using this, we obtain the following equation of motion

$$m\ddot{x} + c_0\dot{x} + (k_0 + k_1)x = k_1 x_s + w(t) \tag{1}$$

where $w(t)$ is a forcing function due to external disturbances. Note that resetting of the spring increases the stiffness, but also in effect moves (or resets) the unstretched length of k_1 spring. The term on the right-hand side is needed since the device can be reset at any time with no injection of energy (e.g. closing of a valve or locking). Without the x_s term, there will be a sudden jump in the total mechanical energy of the system equal to $\frac{1}{2}k_1x^2$, which is not possible with a semi-active device.

As discussed elsewhere [23], a simple application of passivity theorem yields the following control law for $\alpha(t)$ if the device is not to reduce the rate of energy loss in the original system—the structure without the device—(i.e. remain semi-active):

$$\alpha(t)\dot{x}(x_s - x) \leqslant 0, \quad \forall t \tag{2}$$

Since by unlocking the spring (or opening the valve) one can have $\alpha = 0$ at any time, the logic in the expression (2) is fail-safe. The left-hand side is the rate of energy absorbed by the device and, as a result, we wish to avoid setting $\alpha = 0$ as long as expression (2) holds. Furthermore, it is easy to show that once the device is 'reset' (i.e. $\alpha = 1$), the left-hand side of (2) is negative

unless $\dot{x}$ changes its sign. This leads to the following:

$$\begin{aligned} \alpha &= 0, \quad \textit{when } \dot{x} \textit{ changes sign} \\ \alpha &= 1, \quad \textit{as soon as possbile} \end{aligned} \tag{3}$$

where 'as soon as possible' is meant to incorporate the fact that draining of the energy stored in the device is not done instantaneously. In [21] and [20], the ideal resetting logic was based on the assumption that the device can be reset immediately. The control logic in Equation (3) retains the semi-active property while addressing this important practical consideration. We will discuss this further in Section 4.

Finally, we briefly discuss the generalization to a multi-degree-of-freedom structure. Following the steps in [23], relying on generalized coordinated z, and using x as the displacement along the length of the device, we obtain the exact logic as in Equation (3) for each device. Equivalently, the control logic in Equation (3) can be considered as a device-based result; i.e. to ensure that the device does not transfer energy back into the structure, Equation (3) should hold for each device. Note that this gives a decentralized implementation that requires local measurements; namely the rate of change for the displacement along the length of the actuator. Additionally, the logic does not depend on the structural properties and is thus robust to potential modeling errors. Naturally, selecting a suitable size for such devices would require some general understanding of the range of stiffnesses needed.

3. PROTOTYPE DEVELOPMENT

In this Section, we discuss several prototypes that are under testing and evaluation. These prototype devices employ pressurized nitrogen. As shown in [21], and further verified by shake-table testing (see further below and [24]), the force produced by the gas can be approximated by a linear spring with the stiffness $k_1 = 2A^2\kappa p_0/v_0$. Here, A is the piston area, p_0 is initial pressure, v_0 is the initial volume, and κ is the ratio of constant pressure specific heat of the gas to constant volume specific heat (c_p/c_v) of the gas. It was assumed for this derivation that p_0 and v_0 are equal on both sides of the piston.

Our hardware implementation of this device is shown in Figure 2. The cylinder is a Parker hydraulic cylinder capable of a peak pressure of 5000 psi (34.4 MPa) with a 4 inch (10.16 cm)

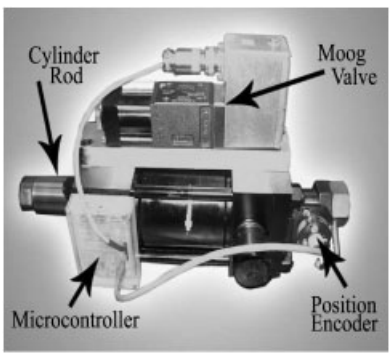

Figure 2. Variable stiffness device capable of 30 000 lb (120 kN) output.

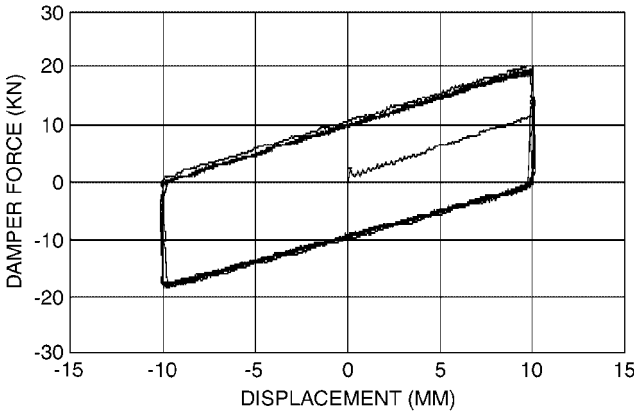

Figure 3. Hysteresis loop of a prototype device.

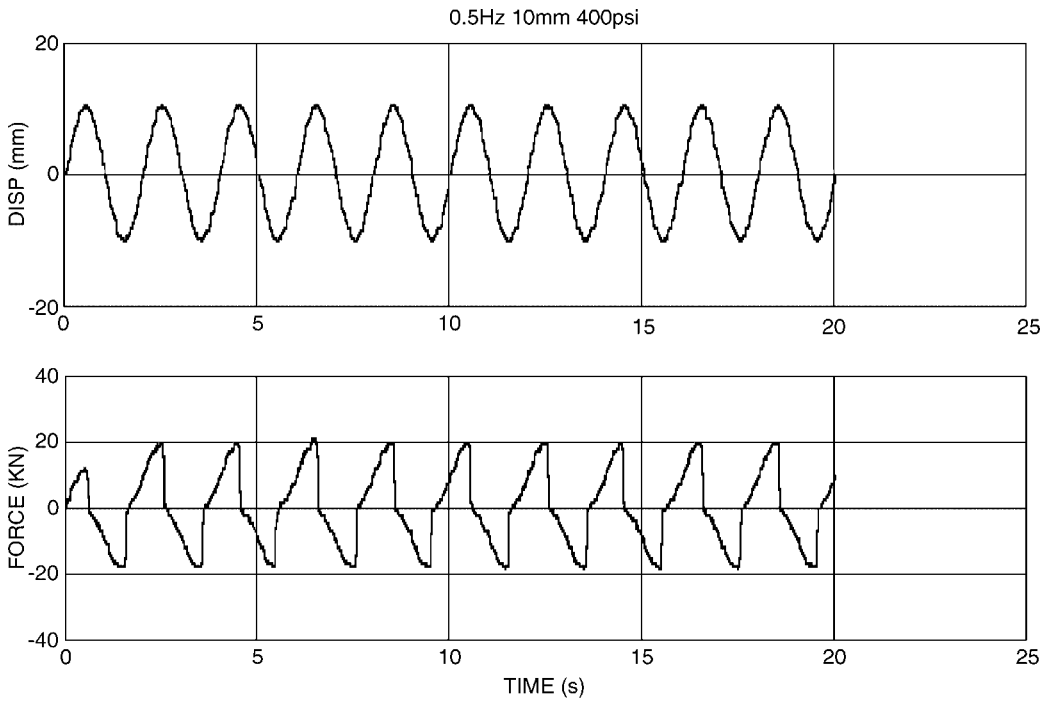

Figure 4. Displacement and force vs time.

bore and a ± 1.5 inch (± 3.8 cm) stroke. The valve connecting the two sides of the cylinder is a Moog direct drive proportional valve capable of less than 10 ms response times with the orifice area proportional to the control voltage. We filled both sides of the hydraulic cylinder with nitrogen gas up to about $p_0 = 600\,\mathrm{lb/inch^2}$ (55 atmospheres). Note that standard hydraulic

cylinders can handle up to 3000 psi (20.64 MPa), so that peak force level of about 30 000 lb (or 120 kN) can be achieved with this device.

Next, we discuss some of the preliminary tests conducted at the National Center for Research on Earthquake Engineering (NCREE) in Taiwan (see [24] for more details). Figure 3 shows the hysteresis loop for one of these devices. This figure shows a consistent and repeatable stiffness that is quite close to a linear spring of roughly 900 kN/m. The rapid drops at the left- and right-hand side of the plot correspond to the 'resetting' of the device; i.e. the valve opens and closes, as the displacement along the damper reverses direction. This is more clear in Figure 4, which shows displacement (top) and device force (bottom) as a function of time. The plots are consistent with a linear spring-like resistance, except at the extreme ends of strokes, when the velocity is changing direction and the resulting resetting reduces the stiffness rapidly.

As the control logic in Equation (3) shows, we would like to finish resetting of the device as soon as possible. By carefully examining the force (or pressure) vs time as the valve is opened, we can estimate the time it takes before we can reset. Experimental data indicates a period of roughly 40 ms for this process, a number consistent with our previous data from different and smaller devices [21]. In the simulation results presented below, we use this number for the delay between setting $\alpha = 0$ and when it is reset to $\alpha = 1$.

4. SIMULATION DETAILS

All simulations were run at a sampling rate of 0.001 s, using the linear isolation system provided, and the eight default bearing locations. Two devices were placed at each bearing location, for a total of sixteen. These devices are all identical and operate as linear springs during non-resetting times. The associated spring constant is $k = 1750\,\mathrm{kN/m}$. Each device requires a single sensor to operate. This sensor may be a velocity sensor or a position sensor, because either can be used to sense a sign change in piston velocity. Since the prototype devices discussed above use a position sensor for feedback, we used the position feedback in the model as well. The control algorithm looks for peaks in the position signal to infer a change in the sign of the velocity. To counter potential difficulties with sensor noise, a threshold is used. As a result, for the damper to reset at a given time, the current position of the piston must be at least 12 mm below the maximum position achieved or 12 mm above the minimum position achieved, depending on whether a high peak or a low peak (a valley) has been detected. This threshold value is relatively small compared with a typical displacement from one peak to the next, which can be 20–60 times larger. In the presence of noise and chatter, it helps prevent the detection of an erroneous or undesirable peak. For the simulation results presented here, we have added a small amount of noise to the signals, in order to demonstrate the robustness of the controller, and to represent measurement uncertainty. This noise is generated by the band-limited white noise block provided by Simulink, and the 'noise power' parameter has been selected such that, on the average, the noise signals have a root-mean-square value of 2 mm.

When the criteria for a peak detection have been met, there is a 20 ms delay before anything happens. This simulates the time it takes for the valve to fully open. After the delay, the pressures on both sides of the piston begin to equalize. This also takes about 20 ms, bringing the total reset time to 40 ms. We modeled the pressure equalization as an exponential decay of

the force F exerted by the piston. Since $F = kx$, where x is relative to the zero-force position (i.e. x_s), this force decay can be brought about by gradually changing x_s to the current value of x. To implement the resetting of x_s, we designed a transfer function, $g(s) = \left(\frac{1}{0.002s+1}\right)$, that tracks a step input to within 0.02% after 20 ms. By inputting the current position to $g(s)$, we can obtain a zero-force position that gives the desired exponential force decay. After this decay is completed, the zero-force position is held fixed; i.e. the device is reset, until the next resetting period. This total of 40 ms delay is consistent with the experimental results on the prototypes [24], as well as the smaller devices discussed elsewhere [21]. As discussed below, we did the simulation for three values of total delay; zero (i.e. ideal), 40 and 80 ms.

5. SIMULATIONS RESULTS

We now present the simulation results along with a brief comparison with results of the clipped optimal control (COC) sample controller [9]. For brevity, we only show the results obtained for the nominal stiffness (i.e. $k = 1750\,\text{kN/m}$), delay (40 ms) and noise levels discussed in the previous section. Using zero delay improves the results slightly, and the conservative value of 80 ms resulted in changes of less than 1%. Similarly, changing the stiffness, which in practice is accomplished by changing the operating pressure, from 50% nominal to 150% nominal did not alter the results qualitatively (i.e. some individual entries would get smaller while others would be larger, with no discernable advantage). In practice, the size of the device is dictated more by the available hardware (i.e. size of the cylinder, pressure).

Tables I and II show the results obtained, presented with a format similar to the one used in [9]. In both tables, 'reset-off' denotes the fail-safe mechanism where the device is not reset and the valve is closed. Note that in this case, in practice the fluid in the chambers will have some viscous damping, which is not modeled in the simulation here. Consequently, the results shown for the passive case underestimate the benefits of this fail-safe mode, and comparisons with semi-active or active forms would be somewhat unrealistic, since the passive mode of resetting is a conservative element—stiffness only—that does not extract any energy.

The second row for each earthquake, denoted by 'reset-active', corresponds to results obtained with the semi-active control of resettable devices while the third row is the results obtained from MR-based clipped optimal control (as a baseline comparison). The results in Tables I and II show somewhat similar overall performance in the sense that in some cases resetting has better performance while in others COC has better performance. Despite this similarity, there are some discernible differences.

First, note that the entries associated with J_6 and J_9 are smaller for the resetting in all cases, i.e. the values for these indices for resetting devices are smaller than those obtained from COC. These indices are related to the peak force of the dampers and the energy absorbed by them. As observed from Tables I and II, the resetting scheme performs better in several cases, with respect to other critical variables (peak interstory displacement or floor acceleration). In such cases, this can be interpreted that the proposed approach is an efficient form of energy removal.

Next, consider the three key indices of J_4, J_5 and J_8 (related to peak inter-storey drift, floor acceleration and acceleration RMS). The overall performance is comparable to that of COC. For example, the results for El Centro are better with resetting, while COC performs better for the Erizinkan record. Averaging the entries of the whole table associated with these indices

Table I. Comparison among three cases: resetting devices always set to high (reset-off), semi-active control of resetting devices (reset-active), and semi-active or clipped optimal implementation of LQG (coc) (FP-x,FN-y).

Earthquake	Case	J_1	J_2	J_3	J_4	J_5	J_6	J_7	J_8	J_9
Newhall	Reset-off	0.99	1.01	0.79	1.15	1.12	0.15	0.75	1.16	0.00
	Reset-active	0.99	1.01	0.67	0.98	1.05	0.22	0.40	0.76	0.67
	LQG (coc)	0.97	1.02	0.56	1.04	1.49	0.30	0.33	0.89	0.79
Sylmar	Reset-off	1.26	1.25	1.18	1.14	1.20	0.14	1.14	1.30	0.00
	Reset-active	1.06	1.08	0.92	0.98	1.15	0.23	0.56	0.81	0.71
	LQG (coc)	0.90	0.91	0.73	0.87	1.16	0.24	0.45	0.74	0.81
El Centro	Reset-off	1.29	1.30	1.00	1.21	1.16	0.16	1.04	1.18	0.00
	Reset-active	1.09	1.07	0.48	0.93	0.96	0.24	0.40	0.61	0.69
	LQG (coc)	1.25	1.23	0.54	1.26	1.61	0.38	0.41	0.76	0.65
Rinaldi	Reset-off	1.30	1.23	1.09	1.22	1.14	0.13	1.10	1.37	0.00
	Reset-active	1.13	1.13	0.76	1.11	1.12	0.23	0.51	0.76	0.69
	LQG (coc)	1.05	1.02	0.60	0.97	1.03	0.27	0.38	0.72	0.77
Kobe	Reset-off	1.13	1.15	0.89	1.21	1.21	0.15	1.01	1.25	0.00
	Reset-active	1.00	0.99	0.51	0.93	1.09	0.23	0.42	0.66	0.65
	LQG (coc)	1.04	1.03	0.52	0.99	1.63	0.28	0.26	0.73	0.73
Jiji	Reset-off	1.11	1.11	1.02	1.10	1.10	0.14	1.08	1.29	0.00
	Reset-active	0.94	0.94	0.67	0.95	0.97	0.23	0.52	0.78	0.62
	LQG (coc)	0.84	0.84	0.65	0.86	0.87	0.17	0.46	0.72	0.64
Erizinkan	Reset-off	1.19	1.21	0.99	1.10	1.15	0.14	1.06	1.26	0.00
	Reset-active	1.10	1.11	0.56	0.94	1.12	0.24	0.50	0.71	0.72
	LQG (coc)	0.93	0.93	0.47	0.86	1.23	0.25	0.34	0.63	0.80

would show a small improvement in the resetting, indicating an effective performance by the resetting devices, though this improvement is mostly due to the El Centro earthquake in which the resetting shows large improvements in acceleration related indices. This is particularly true in J_5 (peak acceleration), which is consistent with the discussion in [21], in which the benefits of the resetting approach was discussed. It is worthwhile to note that resetting results in a more uniform set of values and smaller variations in the resulting indices that COC does. This is particularly true for J_5 for which all values for resetting are within 20% of nominal (i.e. 1.0) while the range for COC is considerably larger (with several entries 60–90% above nominal).

As Tables I and II indicate, the performance of the proposed approach is quite comparable to that of COC. The most important advantages, however, are the simplicity of hardware and software requirements. The controller, as discussed earlier, is simple and decentralized and this can be implemented locally with ease. It does not require central processing, multiple sensors and thus is not subject to traditional reliability concerns. The damper itself employs standard and reliable pneumatic and hydraulic technologies that are inexpensive and easy to maintain.

Table II. Comparison among three cases: resetting devices always set to high (reset-off), semi-active control of resetting devices (reset-active), and semi-active or clipped optimal implementation of LQG (coc) (FP-y,FN-x).

Earthquake	Case	J_1	J_2	J_3	J_4	J_5	J_6	J_7	J_8	J_9
Newhall	Reset-off	0.93	0.99	0.83	1.12	1.12	0.14	0.89	0.90	0.00
	Reset-active	0.89	0.92	0.65	1.09	1.11	0.20	0.54	0.79	0.66
	LQG (coc)	0.88	0.92	0.55	1.24	1.40	0.30	0.42	0.84	0.79
Sylmar	Reset-off	1.33	1.31	1.25	1.23	1.22	0.14	1.21	1.28	0.00
	Reset-active	0.94	0.92	0.86	0.90	0.96	0.24	0.61	0.70	0.71
	LQG (coc)	0.81	0.79	0.74	0.79	0.92	0.23	0.51	0.61	0.81
El Centro	Reset-off	1.26	1.26	1.06	1.56	1.29	0.15	1.01	1.43	0.00
	Reset-active	1.10	1.10	0.67	1.10	1.10	0.21	0.48	0.80	0.68
	LQG (coc)	1.26	1.25	0.65	1.41	1.93	0.37	0.45	0.94	0.70
Rinaldi	Reset-off	1.13	1.11	1.21	1.15	1.15	0.14	1.13	1.13	0.00
	Reset-active	1.05	1.10	0.70	1.13	1.14	0.22	0.46	0.54	0.69
	LQG (coc)	0.98	1.01	0.62	0.99	1.02	0.26	0.30	0.47	0.78
Kobe	Reset-off	1.26	1.26	0.84	1.27	1.24	0.15	1.06	1.41	0.00
	Reset-active	1.21	1.21	0.60	1.22	1.17	0.22	0.46	0.80	0.65
	LQG (coc)	1.15	1.20	0.53	1.33	1.47	0.30	0.38	0.98	0.71
Jiji	Reset-off	1.12	1.12	0.98	1.10	1.10	0.15	1.22	1.35	0.00
	Reset-active	0.83	0.83	0.63	0.84	0.91	0.24	0.54	0.74	0.62
	LQG (coc)	0.74	0.73	0.63	0.73	0.80	0.17	0.46	0.61	0.64
Erizinkan	Reset-off	1.23	1.23	0.97	1.23	1.23	0.14	0.96	1.19	0.00
	Reset-Active	1.00	0.99	0.58	1.03	1.09	0.24	0.43	0.60	0.73
	LQG (coc)	0.85	0.84	0.51	0.88	1.16	0.24	0.32	0.52	0.78

6. CONCLUSIONS

A new semi-active device that manipulates stiffness properties is presented. The general approach, the control logic and preliminary experimental results are presented for this device and its performance is evaluated through simulations on the benchmark smart base-isolated building. This resetting device offers overall performance that is competitive with other semi-active devices, along with important advantages in low cost, simplicity and reliance on standard pneumatic or hydraulic techniques.

ACKNOWLEDGEMENT

This research is supported by the National Science Foundation, Grant CMS-0218813.

REFERENCES

1. Yang JN, Danielians A. A seismic hybrid control systems for building structures. *Journal of Engineering Mechanics* (ASCE) 1991; **117**(4):836–853.

2. Yang JN, Li Z, Liu SC. Control of hysteretic systems using velocity and acceleration feedback. *Journal of Engineering Mechanics* (ASCE) 1992; **118**(11):2227–2245.
3. Yang JN, Wu JC, Hsu IR. Control of sliding isolated buildings using dynamic linearization. *Journal of Engineering Structures* 1994; **16**(6):437–444.
4. Yang JN, Wu JC, Agrawal AK. Sliding mode control of nonlinear and hysteretic structures. *Journal of Engineering Mechanics* (ASCE) 1995; **121**(12):1386–1390.
5. Yang JN, Wu JC, Kawashima K, Unjoh S. Hybrid control of seismic excited bridge structures. *Journal of Earthquake Engineering and Structural Dynamics* 1995; **24**(11):1437–1451.
6. Spencer B, Johnson EA, Ramallo J. Smart base isolation for seismic control. *JSME International Journal*, *Series C* 2002; **43**(3):704–711.
7. Ramallo J, Johnson EA, Spencer B. Smart base isolated systems. *Journal of Engineering Mechanics* (ASCE) 2002; **128**(10):1088–1099.
8. Narasimhan S, Nagarajaiah S, Johnson EA, Gavin HP. Smart base isolated benchmark building part I: problem definition. *Journal of Structural Control and Health Monitoring* 2006.
9. Nagarajaiah S, Narasimhan S. Smart base isolated benchmark building part II: phase I sample controllers for linear isolation systems. *Journal of Structural Control and Health Monitoring* 2006.
10. Symans MD, Kelly SW. Fuzzy logic control of bridge structures using intelligent semi-active seismic isolation. *Earthquake Engineering and Structural Dynamics* 1999; **28**:37–60.
11. Yang JN, Agrawal AK. Semi-active hybrid control systems for nonlinear buildings against near-field earthquakes. *Journal of Engineering Structures* 2002; **24**:271–280.
12. Nasu T, Kobori T, Takahashi M, Niwa N, Ogasawara K. Active variable stiffness system with non-resonant control. *Earthquake Engineering and Structural Dynamics* 2001; **30**:1598–1614.
13. Kobori T, Takahashi M, Nasu T, Niwa N, Ogasawara K. Seismic response controlled structure with active variable stiffness system. *Earthquake Engineering and Structural Dynamics* 1993; **22**:925–941.
14. Nagarajaiiah S, Mate S. Semi-active control of continuously variable stiffness system. *Proceedings of the 2nd World Congress on Structural Control*, Kyoto, Japan, 1998; **1**:397–406.
15. He WL, Agrawal AK, Yang JN. Novel semiactive friction controller for linear structures against earthquakes. *Journal of Structural Engineering* 2003; **129**(7):941–950.
16. He WL, Agrawal AK. Applications of several semi-active control systems to the benchmark base-isolated building. *Proceedings of the ASCE Engineering Mechanics Conference*, Newark (DE), June 2004; CD-ROM.
17. Spencer B, Nagarajaiah S. State of the art of structural control. *ASCE Journal of Structural Engineering* 2003; **129**(7):845–856.
18. Bobrow JE. High performance damping with a semi-active spring. *1997 ASME Design Technical Conferences*, Sacramento, CA, September 1997; DETC97/VIB-3826.
19. Bobrow JE, Jabbari F, Thai K. A new approach to shock isolation and vibration suppression using a resetable actuator. *ASME Transactions on Dynamic Systems*, *Measurement and Control* 2000; **122**:570–573.
20. Yang JN, Kim JH, Agrawal AK. A resetting semi-active stiffness damper for seismic response control. *ASCE*, *Journal of Structural Engineering* 2000; **126**(12):1427–1433.
21. Jabbari F, Bobrow JE. Vibration suppression with a resetable device. *Journal of Engineering Mechanics* (ASCE) 2002; **128**(9):916–924.
22. Agrawal AK, Yang JN, He WL. Applications of some semi-active control systems for a benchmark cable-stayed bridge. *Journal of Structural Engineering* (ASCE) 2003; **129**(7):884–894.
23. Leavitt J, Jabbari F, Bobrow JE. Control and performance of variable stiffness devices for structural control. *ACC-05*, June 2005.
24. Yang JN, Boborw J, Jabbari F, Cheng CP, Lin PY. Full scale experimental verification of resetable semi-active stiffness damper. *Proceedings of the Second ANCRiSST Workshop on Advanced Smart Materials and Smart Structures Technology*, July 21–24, 2005, Gyeongu, Korea (in press).

